Computers in Biology and Medicine 197 (2025) 111026

Contents lists available at ScienceDirect

Computers in Biology and Medicine

journal homepage: www.elsevier.com/locate/compbiomed

Highly reliable personalized noninvasive hemoglobin estimation by using Vision Transformers and dual fine-tuning

Mauro Camporeale [a], Felice Clemente [b], Giovanni Dimauro [a,*], Nunzia Lomonte [a], Rosalia Maglietta [c], Crescenza Pasciolla [b], Davide Sacco [a], Gian Maria Zaccaria [b]

[a] University of Bari "Aldo Moro", Department of Computer Science, Bari, Italy
[b] U.O.C. Ematologia e Terapia Cellulare, IRCCS Istituto Tumori "Giovanni Paolo II", Bari, Italy
[c] Department of Electrical and Information Engineering (DEI), Polytechnic University of Bari, Bari, Italy

ARTICLE INFO

Keywords:
Artificial intelligence
Anemia detection
Precise medicine
Vision Transformer
Medical imaging
Personalized medicine

ABSTRACT

Artificial intelligence is revolutionizing health care, particularly in precision medicine and noninvasive diagnostics. Anemia, which is a widespread condition that affects billions of people worldwide, compromises oxygen transport due to low hemoglobin levels, which leads to severe complications if left undetected. Early and frequent monitoring is essential, yet traditional blood tests can be invasive, costly, and impractical for continuous assessment. This study presents the first patient-specific system for noninvasive hemoglobin estimation from palpebral conjunctiva images. Unlike previous approaches, our model integrates the vision transformer (ViT) architecture with dual fine-tuning, which enables personalized adaptation to each patient's unique physiological characteristics. The dataset consists of conjunctival images captured over multiple days from the same patients, which allows for an individualized calibration process that enhances predictive accuracy. Our model achieved an R2 of 0.94, an accuracy of 98%, and a mean absolute error (MAE) of 0.25 g/dL, thus demonstrating a performance comparable to that of laboratory tests. Additionally, the model's 100% sensitivity ensured that all anemic cases were detected, thereby minimizing the risk of false-negatives. By providing highly precise, rapid, and accessible anemia screening, this approach has the potential to redefine long-term hematological monitoring, thereby reducing reliance on frequent blood tests and improving clinical decision-making in resource-limited settings.

1. Introduction

Anemia is a widespread health issue that affects individuals in both developed and developing countries. It results in a decrease in blood hemoglobin(Hb) levels and has significant implications for human health. According to the World Health Organization(WHO), anemia affects more than a billion people globally, with varying degrees of severity [1–5]. Clinically, anemia is defined as a condition where there is a lower than normal number of red blood cells or Hb concentration within them. If a patient has a deficiency of red blood cells or Hb, or if their red blood cells are abnormal, their ability to carry oxygen to the body's tissues is reduced. This can result in symptoms such as fatigue, weakness, dizziness, and shortness of breath. Anemia caused by deficiencies in iron, vitamin B12, folate, or Hb can lead to abnormal or altered production of erythrocytes [6]. When Hb levels are above 9–10 g/dL, symptoms may not be apparent because the body tries to compensate for the loss. For example, the heart rate may increase in response to hypoxia. However, when this compensation is no longer sufficient to provide adequate oxygen levels, the aforementioned symptoms may appear.

According to the WHO [1], accurately detecting anemia and determining its overall impact worldwide are challenging, even in more economically developed regions. All countries must bear the costs of managing this disease, including the cost of prevention (or lack thereof), traditional analysis equipment, administration, and accommodation. Additionally, it is difficult to estimate the financial and social costs for patients with anemia. Some patients may require frequent laboratory testing, which can be uncomfortable because of repeated blood draws and may incur additional costs for transportation and/or assistance. Mass screening is also not feasible in developing countries, particularly in areas with limited economic resources, due to the lack of noninvasive and cost-effective diagnostic methods. To obtain a definitive diagnosis, a careful study of the patient's medical history and physical and instrumental examinations are needed. During the physical examination, the heart and respiratory rates are recorded, and

* Corresponding author.
E-mail address: giovanni.dimauro@uniba.it (G. Dimauro).

https://doi.org/10.1016/j.compbiomed.2025.111026
Received 9 May 2025; Received in revised form 14 August 2025; Accepted 28 August 2025
Available online 6 September 2025
0010-4825/© 2025 The Authors. Published by Elsevier Ltd. This is an open access article under the CC BY-NC-ND license (http://creativecommons.org/licenses/by-nc-nd/4.0/).

the pallor of exposed tissues is evaluated. Blood sample analysis is then used to provide a definitive diagnosis of anemia. Many studies have been conducted to establish whether direct examination of the exposed tissue by the physician is sufficiently reliable for identifying anemia. The results are rather controversial, but many authors agree that direct examination is reliable only for cases of severe anemia and that its reliability depends on the doctor's experience and the use or nonuse of aids as color-tint selectors.

In recent years, interest among researchers in developing noninvasive and cost-effective methods and tools for monitoring hemoglobin levels for both laboratory and home use has increased. Several recent studies have focused on the development of desktop and multi-platform applications that allow clinicians to remotely monitor patients' hematological parameters, thereby facilitating continuous follow-up and reducing the need for in-person visits [7,8]. Doctors can suspect anemia on the basis of examinations of the palms of the hands, fingertips, nail beds, tongue, and eye conjunctiva, but the diagnosis is not certain. As a result, devices and methods that can diagnose anemia by capturing images of these body areas in a noninvasive, cost-effective, and easily accessible manner are needed. Research into the automatic diagnosis of anemia via noninvasive techniques is relatively new, and there are no shared datasets available for comparing different approaches. Each research group has worked with their own data, sometimes on small datasets or without specifying the experimental setup, and nontrivial issues such as the influence of ambient light during image capture have not been addressed. Additionally, some studies have used complex and expensive equipment that is not suitable for large-scale industrial development. In [9], the authors identified several open problems, including (a) which part of the conjunctiva provides the best results for estimating anemia; (b) how many digital images of one or both eyes are needed for a reliable evaluation; (c) the lack of a shared dataset; and (d) the lack of low-cost devices suitable for widespread use.

This work presents a novel, noninvasive, and patient-specific approach for automated hemoglobin estimation by deep learning. Unlike previous methods, our method personalizes predictions for each individual by leveraging the vision transformer (ViT) architecture with dual fine-tuning. By utilizing conjunctival images, our model provides an accurate, accessible, and cost-effective alternative to traditional blood tests.

Our approach involves a multistep pipeline to ensure optimal model performance. First, we collected a comprehensive dataset of conjunctival images, which were preprocessed and segmented using a U-Net network. The segmented images were resized via bilinear interpolation to match the input dimensions of Google's pretrained ViT-Base-Patch16-224 model. The training was conducted in two sequential fine-tuning phases:

1. For general fine-tuning, the pretrained ViT model was adapted to predict hemoglobin levels from conjunctival images.
2. For patient-specific fine-tuning, the model was further refined by using images from a single patient to improve personalized predictions.

To ensure robust model evaluation, we implemented a leave-one-out validation strategy at both fine-tuning stages. Initially, the generalized model was trained while one patient per cycle was excluded. In the second phase, the excluded patient's images were used for individual fine-tuning, with one image left out for final testing. This iterative process optimized both generalization and personalization, which enabled the model to deliver highly accurate and individualized predictions.

By incorporating soft calibration at the patient level, this study advances the field of noninvasive hemoglobin estimation by offering a scalable and clinically viable tool for continuous anemia monitoring.

The remainder of this paper is structured as follows: Section 2 provides a review of the literature on anemia diagnosis through the analysis of conjunctival images and the use of cost-effective, noninvasive devices in previous research. Section 3 describes the device and datasets used in this study. In Section 4, we present the experiment conducted. Finally, Section 5 presents the results and discussion.

2. Related work

Noninvasive devices are medical instruments that perform their functions without penetrating the skin or any body openings. These devices can be used for a variety of purposes, including diagnosis, monitoring, treatment, and prevention of various health conditions.

Young et al. [10] reported that noninvasive devices have poorer performance than invasive devices do but noninvasive devices are considered highly acceptable and easy to use. They claim that noninvasive technologies have the potential to transform anemia screening in low-resource settings.

A comprehensive review of noninvasive anemia detection techniques [9] identified key challenges in existing projects. The authors provide a structured roadmap for researchers in the field and emphasize the importance of dataset quality and image acquisition as critical factors for success. Similarly, a 2023 review by Appiahene et al. [11] confirmed that dataset quality and size remain major obstacles in noninvasive anemia detection research.

2.1. Palpebral conjunctiva

Among the various noninvasive methods explored, conjunctiva imaging has gained significant attention because of its strong correlation with hemoglobin levels, as discussed in the following section. Previous studies have shown that conjunctival images provide more reliable results than other anatomical images do, such as images of fingertips or nail beds [12–14]. External factors such as skin thickness variations from manual labor and color changes in nails due to nutritional deficiencies can affect measurements. Thus, the conjunctiva is a more stable and accurate region for analysis. Recent research has demonstrated the potential of conjunctiva-based imaging beyond anemia detection. For example, Babenko et al. [15] developed a deep learning model capable of predicting multiple vital signs from a simple image of the external eye, which highlights the high diagnostic value of ocular imaging.

Park et al. [16] presented software that uses imaging of the palpebral conjunctiva to reconstruct high-resolution spectra of blood Hb. They implemented a fixed-design linear regression, namely, a least-squares method, to convert RGB data to spectral data. On the validation set, they obtained an R^2 of 0.912 and a LOA of [-2.20, 2.29 g/dL].

Suner et al. [17] developed an algorithm for predicting hemoglobin concentration via smartphone-captured images of the conjunctiva. They worked with ROW and PNG files to obtain images with high resolution. Twenty-six features were extracted from the images, and a generalized linear model was trained. Finally, they obtained an accuracy of 82.9%, a sensitivity of 90.7% and a specificity of 73.3%.

Anggraeni and Fatoni [18] introduced a noninvasive anemia detection system based on a digital image of the palpebral conjunctiva captured by a smartphone camera. All the subjects were pregnant women. They tried to identify features that can be correlated with the level of hemoglobin. Among the three color (red, green, blue) intensity levels, the red color intensity was highly correlated with clinically measured Hb levels, with $R^2 = 0.8139$.

Ghosal et al. [19] implemented sHEMO, which is an app that can measure conjunctival pallor from captured eye images and can subsequently predict blood Hb levels with an R^2 of 0.8774.

Digital images of the lower palpebral conjunctiva were also obtained by Kasiviswanathan et al. [20]. Their model was trained to perform well under any lighting conditions and without the use of external hardware. They trained a ridge regression algorithm to estimate the hemoglobin level and achieved an mean absolute error (MAE) of 1.34 g/dL and an root mean squered error (RMSE) of 1.72 g/dL.

INAP, which was created by Ghosal et al. [21], is a system that combines a photograph of the conjunctiva and a photograph of a fingernail. The ROIs in both photographs are extracted automatically, and the Hb level is computed after the estimation of the dominant color

of each ROI. The model predicts blood hemoglobin with an accuracy of 0.33 g/dL, a bias of 0.2 g/dL and a sensitivity of 90%.

Dimauro et al. [22] collected for the first time a dataset of photographs of eyes from patients of two different ethnicities: Italian and Indian. RUSBoost was applied to 14 features to predict anemia. It was shown that datasets that contain images of people of different ethnicities can result in different performance values, so it is important to have photographs of people of different ethnicities. The final accuracy, sensitivity and specificity on the joint dataset were 83%, 69% and 87%, respectively.

The study by Appiahene et al. [23] provided a dataset called CP-AnemiC, which contains photos of 710 individuals, both anemic and nonanemic. This study aimed to classify anemia and perform regression on the amount of Hb in the blood using deep neural networks such as ResNet50 and DenseNet121. The results revealed a maximum accuracy of 84.79% for classification and a MAE of 1.50 for regression.

In [24], the authors proposed a method for extracting the most prominent vessels in the sclera from eye images. The segmentation process yielded very satisfying results. Afterward, they extracted 10 color features to perform classification on hemoglobin concentration levels. The best results, with an accuracy of 86.4%, were obtained with SVM with color features from the whole sclera.

Kato et al. [25] developed machine learning and deep learning models for predicting hemoglobin levels from 150 palpebral conjunctiva images captured with a smartphone. A convolutional neural network (CNN)-based model achieved a correlation of 44% between actual and predicted hemoglobin values, with a sensitivity of 20% and a specificity of 99% for anemia detection. The model's accuracy improved slightly after the aspect ratio and exposure time of the images were corrected. The activation maps indicated that the lower conjunctiva plays a crucial role in hemoglobin level estimation.

Among the existing approaches, the study by Das et al. [26] represents the first application of the ViT model for hemoglobin prediction. This study demonstrated its potential for noninvasive anemia screening. This research introduced NiADA, which is a smartphone-based AI application that estimates hemoglobin levels from images of the lower palpebral conjunctiva. The model, which was trained on over 30,000 images, was validated against both laboratory hemoglobin measurements and the HemoCue Hb 301, which is a commonly used point-of-care testing (POCT) device. The study involved 556 participants, including adult males, females, pregnant women, and pediatric patients. The results revealed that the NiADA hemoglobin predictions aligned closely with the laboratory values, with a mean difference that ranged from −0.89 g/dL to 0.61 g/dL depending on the group. The highest specificity (90%) was observed in pregnant women, whereas the highest sensitivity (75.8%) was observed in adult females.

Two interesting projects that focused on the segmentation of the conjunctiva are described as follows: In [27], fine-tuning was performed on the U-Net neural network, and an intersection over union of 85.7% was achieved, whereas in [28], graph partitioning was used for segmentation, which resulted in an accuracy of 93.79%. Both techniques can be used as a first step in creating a model for detecting anemia.

In addition to deep learning approaches, traditional methods like random walk and cantilever beam models [29–31] have been used for contour extraction in medical imaging. Their ability to delineate contiguous regions efficiently may complement DL-based methods in hybrid systems.

3. Materials

To conduct this study, both a dedicated image acquisition device and a well-structured dataset were needed. The following sections describe the design of the device and the characteristics of the dataset used for our experiments.

Fig. 1. Close-up view of the spacer on our device, with the LED turned on.

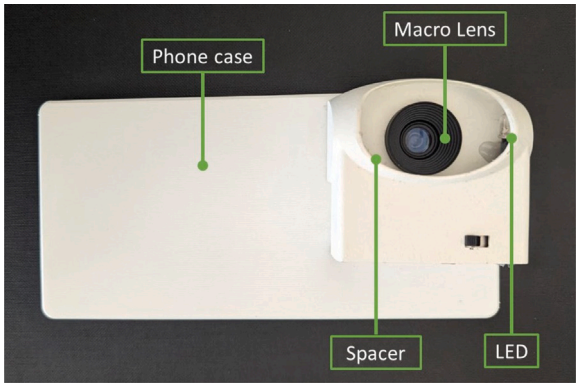

Fig. 2. Device used in this research, with its specific components labeled, including a phone case for attachment, a macro lens for capturing palpebral conjunctiva images, an LED for illumination, and a spacer for proper positioning on the patient's eye.

3.1. Device

A custom-built image acquisition device was developed at the Computer Science Department of the University of Bari. The goal was to design a system that would enable high-quality, standardized imaging of the palpebral conjunctiva using a smartphone. The system consists of an external phone case with a *spacer* which was specifically designed for the smartphone used for all image acquisitions. The case and spacer were *3D-printed*, and multiple tests were conducted to determine the optimal configuration for our study.

Within the spacer, two key components ensure uniform image quality:

1. A *Selvim 25X 4K HD macro lens* enables high-resolution close-up capture of the conjunctiva.
2. A set of *5 mm white LED lights* provides consistent illumination and eliminates the need for the phone's built-in flash by ensuring uniform lighting conditions across all images.

To maintain imaging consistency, the camera was set to PRO mode to enable manual control of the shutter speed, aperture, and ISO settings, which remained constant throughout the study.

The white color of the device helps diffuse the LED light evenly. Fig. 1 shows the device in operation, with the LED turned on. The shape of the spacer allows for correct positioning of the patient's eye without causing discomfort. The image capture time is very short, namely, approximately 1 s. A detailed image of the final device is presented in Fig. 2.

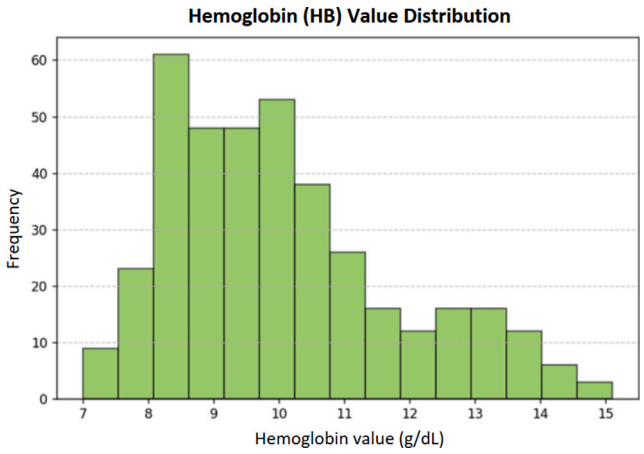

Fig. 3. Frequency distribution of hemoglobin values in the dataset, which highlights the main concentration between 8 and 11 g/dL.

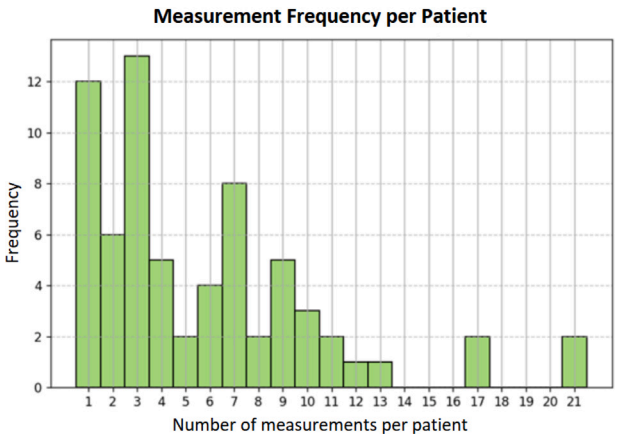

Fig. 4. Distribution of the number of hemoglobin measurements per patient in the dataset, which illustrates the variability in the measurement frequency.

3.2. Dataset

Our dataset was created in collaboration with the "Istituto Tumori Bari Giovanni Paolo II" hospital in Bari. The photos were taken from May to November 2023 and from May to August 2024. We selected patients from the hematology ward as our study population since they had various conditions that affect hemoglobin levels, such as leukemia and coagulopathies. The data collection was conducted following the approval of the study protocol by the Ethics Committee of the Giovanni Paolo II Institute (Prot. n. 691/CE dated 22/12/2022). With the patients' informed consent, we photographed their palpebral conjunctiva — the inner lining of the eyelid — immediately before or after their routine blood draw, all conducted during the same clinical session in the morning. This strict temporal alignment ensured that each image could be reliably associated with the corresponding hemoglobin value measured from the venous blood sample, allowing for a consistent and accurate analysis of the visual-to-physiological correlation.

The patients were aged between 20 and 70 years, with a sex distribution of 56% male and 43% female. The shape and size of the conjunctiva varied from patient to patient, with some having a more spacious and evident conjunctiva, whereas others had smaller conjunctiva with more pronounced scleral blood vessels. This made our dataset generalizable and capable of capturing all types of palpebral conjunctiva.

With respect to hemoglobin levels, the dataset was skewed toward low hemoglobin values, which is expected for a population with a high prevalence of anemia or hematological disorders. As shown in Fig. 3, the hemoglobin values were primarily between 8 and 11 g/dL. Moreover, 324 individuals had hemoglobin levels below 12 g/dL, which confirmed an overall trend toward low hemoglobin levels in the dataset.

In terms of measurement frequency, each patient had an average of 5.69 measurements, as shown in Fig. 4. The maximum number of recorded measurements for a single patient was 21, whereas some patients had only one measurement. The distribution of the number of measurements suggests that certain patients underwent more frequent clinical monitoring than others did.

All the data acquired are protected by privacy laws, and we could use only information about the pathology, sex, and age of each patient.

In total, we collected images from 109 patients, with a total of 436 photos. Examples of images from this dataset can be found in Fig. 5. This dataset provides diverse and representative samples for training and evaluating our hemoglobin prediction model. The combination of controlled image acquisition and patient variability ensures robustness in real-world applications.

4. Methods

In this section, we provide a detailed description of the methodology and steps applied to achieve the objectives of this study. All operations were performed using Python 3.11.9 with Visual Studio Code as the integrated development environment (IDE). The key libraries included NumPy [32], Pandas [33], Torchvision [34], and Transformers [35].

4.1. Preprocessing

The role of preprocessing in medical image-based diagnostics is crucial. As discussed in [36] and [37], proper image standardization and segmentation significantly affect model robustness. The objectives of this step were to improve the quality of the data and to convert them into the appropriate format for the model. Initially, all captured images were manually reviewed, and few samples affected by blur, suboptimal eye opening, or incorrect positioning were excluded to ensure data quality and consistency. The cleaned dataset was then used for further processing. The second step involved isolation of the lower part of the conjunctiva, which was the area of diagnostic interest for hemoglobin level prediction. This was an essential step for ensuring accurate prediction. To achieve this, it was necessary to manually intervene for a subset of the images by cropping them to create a dataset suitable for training the U-Net network. This process provided the model with clear and well-defined examples of the region to be segmented, which enhanced its accuracy and generalizability. The U-Net network was chosen for segmentation on the basis of the work presented in [27]. Fig. 6 shows the final result of this algorithm for an image from our dataset.

The next step was to check the dataset; one of the main challenges encountered was the imbalanced nature of the dataset. Since certain ranges of hemoglobin values were overrepresented, the model could have learned to favor those values, which would have compromised the generalization of the predictions. To mitigate this issue, sampling was performed by removing some images with the more represented values. This allowed for a more homogeneous distribution, which improved the model's ability to learn real correlations between the appearance of the conjunctiva and hemoglobin levels. In the end, only 125 photographs were used for training. The number of observations for a single hemoglobin value was reduced from over 25 to a maximum of 12, as shown in Fig. 7, in line with the various observed value ranges. In the final step, to ensure compatibility with the pretrained model, all the images were resized to 224 × 224 pixels using bilinear interpolation.

Fig. 5. Four images of the palpebral conjunctiva of four different patients from the hematology ward of the "Istituto Tumori Bari Giovanni Paolo II" hospital in Bari.

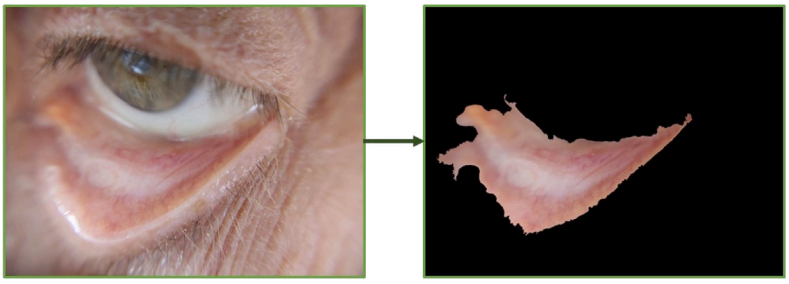

Fig. 6. An example of the segmentation process applied to an image from the dataset, showing the original image and the segmented palpebral conjunctiva.

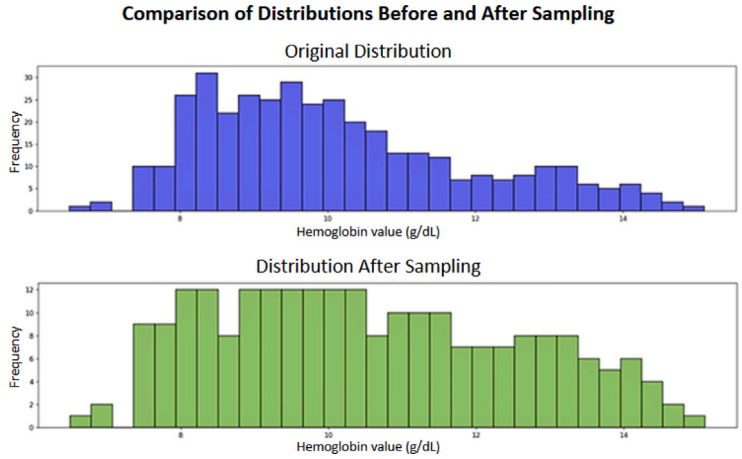

Fig. 7. Comparison of hemoglobin value distributions before and after sampling. The original distribution (top) shows an overrepresentation of certain hemoglobin values. The adjusted distribution (bottom) demonstrates a more uniform representation of hemoglobin values, which enhanced the model's ability to learn meaningful correlations between conjunctival appearance and hemoglobin levels.

4.2. Training and testing

For the training phase, we used the ViT-based patch16-224, which is a vision transformer model pretrained on ImageNet by Google. This model segments an image into small 16 × 16 pixel patches and processes them similarly to a sequence of textual tokens. This approach enables the model to capture spatial relationships between different image regions and learn complex visual patterns. The use of a pretrained model enabled us to leverage features already learned from a large and diverse image dataset, thus improving training efficiency given the limited size of our dataset. Fine-tuning of this pretrained model by adjusting its learned weights on the basis of new examples enabled it to adapt specifically to our dataset. This process refined the model's ability to recognize patterns relevant to our specific application while maintaining the advantages of its prior general training.

Vision Transformers differ fundamentally from convolutional neural networks in their architectural design, lacking inherent spatial inductive biases such as locality and translation invariance. While this absence provides greater modeling flexibility and allows the network to learn spatial relationships directly from data, it can present challenges when working with limited datasets or noisy medical images where these spatial priors would typically be beneficial. To address these architectural characteristics and the inherent constraints of medical imaging datasets, where patients typically have limited conjunctival images available, we developed a strategic methodology designed to minimize both overfitting and underfitting through sequential model adaptation. We implemented a dual fine-tuning approach using the

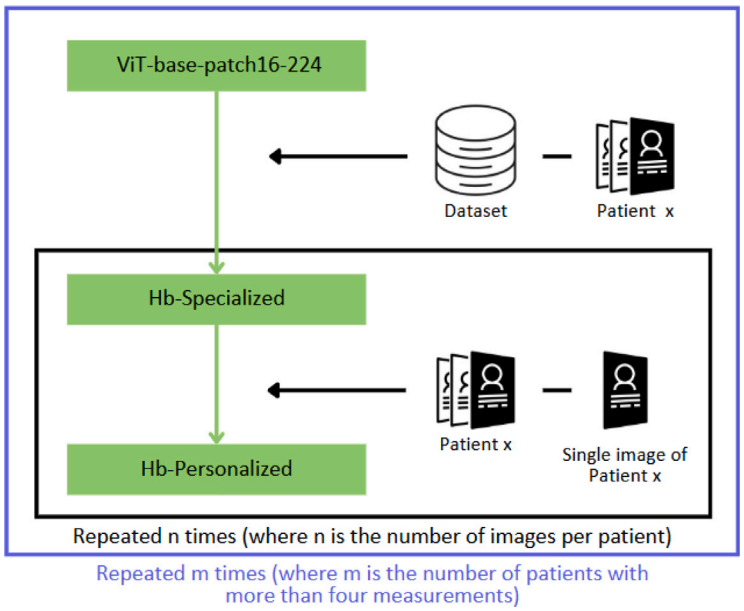

Fig. 8. Overview of the two-step fine-tuning process. The ViT-base-patch16-224 model was first fine-tuned using all images in the dataset except those from one patient, thereby producing the Hb-specialized model. This step, which was repeated m times (once per patient), ensured that the model learned a generalizable representation for hemoglobin prediction. In the second step, the Hb-specialized model was further fine-tuned on all but one image of the previously excluded patient, thus generating the Hb-personalized model. This step was repeated n times (once per image of the patient), which enabled the model to adapt to individual variability and improved the prediction accuracy.

leave-one-out (LOO) technique, which is a widely used validation method in machine learning where one data point is excluded from training and used solely for testing.

The model training process consisted of two distinct phases:

- **General fine-tuning (Hb-specialized model)**: The ViT-based-patch16-224 model was fine-tuned on all the images in the dataset except those of a single patient. This technique ensured that the model did not rely on data from the excluded individual. This phase generated a specialized model for hemoglobin prediction, which is referred to as the Hb-specialized model.
- **Patient-specific fine-tuning (Hb-personalized model)**: The Hb-specialized model was then further adapted for individual patients. This was achieved by performing a second fine-tuning step using all the images of the previously excluded patient except for one image. In this phase, the leave-one-out technique was applied at the image level, with one image excluded at a time. This process was repeated n times, where n n is the number of images available for that patient. The resulting model, which was fine-tuned for an individual patient, is referred to as the Hb-personalized model.

Both fine-tuning stages were repeated m times, where m is the number of patients in the dataset with more than four measurements. The final performance metrics were computed as averages across all iterations. Only patients with at least four images in the dataset were considered for the personalization phase to ensure a more generalized fine-tuning process. The total number of such patients was 25. Fig. 8 provides a graphical representation of the proposed methodology, which shows the transition from general fine-tuning to patient-specific adaptation. This approach was also intended to limit overfitting by ensuring that the model is never trained or evaluated on the same image, and by enforcing generalization across subjects. Additionally, only patients with sufficient image diversity were used for personalized training to enhance robustness.

Fig. 9 provides a visual representation of the variability in hemoglobin levels across patient images. For most patients included in the fine-tuning of the Hb-personalized model, hemoglobin levels fluctuated significantly across different images. This ensures that the model does not predict hemoglobin values correctly merely by memorizing a patient's trend but rather by extracting specific visual features from each photograph. Additionally, the performance metrics were calculated by excluding one image at a time during the second fine-tuning phase. This approach enabled us to evaluate the model's predictive performance across all the images rather than relying on a single random selection.

This approach aims to first develop a generalized hemoglobin prediction model and subsequently personalize it for individual patients, thereby enhancing overall predictive performance.

To evaluate the regression, we used the following performance metrics:

- Mean squared error (MSE): This metric measures the average squared difference between the predicted and actual values and penalizes large errors more than smaller errors.
- Root mean squared error (RMSE): This metric provides a more interpretable error measure by returning the error in the same unit as the predicted variable.
- Mean absolute error (MAE): This metric computes the average absolute difference between the predicted and true values and, thus, is less sensitive to outliers.
- Coefficient of determination (R^2): This metric evaluates how well the model explains the variance in the data, with values closer to 1 indicating a better fit.

To compare our work effectively with the state-of-the-art methods, we needed to compute additional classification metrics. Since our model performs regression, we applied a classification approach in which the predicted hemoglobin values were divided into two distinct categories: *anemic* and *nonanemic*.

Following standard clinical guidelines, we labeled individuals as anemic if their hemoglobin levels were below 12 g/dL for women and below 13 g/dL for men [38]. On the basis of this classification, we calculated key performance metrics to evaluate the model's diagnostic performance:

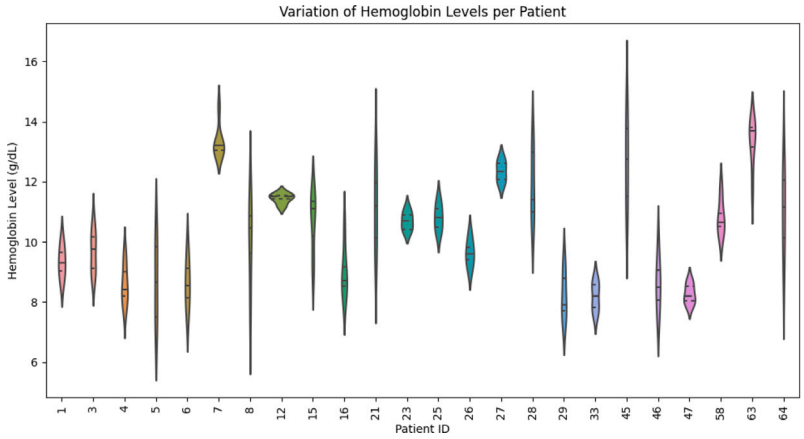

Fig. 9. Analysis of hemoglobin level variability in the images used to fine-tune the Hb-personalized model to ensure that the model does not merely memorize trends but extracts meaningful visual features.

Table 1
Comparison of prediction errors before and after patient-specific fine-tuning.

Error threshold	Hb-specialized	Hb-personalized
Errors > 0.5 g/dL	102	18
Errors > 1.0 g/dL	77	4

- Sensitivity (true positive rate): This metric measures the model's ability to correctly identify anemic individuals. A higher sensitivity indicates that the model effectively detects anemia cases, thus reducing the risk of false-negatives.
- Specificity (true negative rate): This reflects how well the model correctly identifies nonanemic individuals. High specificity ensures that healthy individuals are not mistakenly classified as anemic, thus minimizing false positives.
- Positive predictive value (PPV): Also known as precision, the PPV indicates the probability that a patient classified as anemic by the model is actually anemic. This metric is crucial for assessing the reliability of positive anemia predictions.
- Negative predictive value (NPV): This metric represents the likelihood that a patient classified as nonanemic is truly nonanemic. A high NPV suggests that the model is effective at ruling out anemia when it predicts a normal hemoglobin level.
- Accuracy: This metric measures the overall correctness of the model's predictions by evaluating the proportion of correctly classified cases (both anemic and nonanemic) out of all test samples.

By computing these metrics, we provide a clinically relevant evaluation of our model's ability to diagnose anemia, thereby facilitating direct comparison with existing classification-based approaches in the literature.

5. Results and discussion

Now, we evaluate the accuracy of the predictions, analyze how the model performs under different conditions, and assess variations in weight distributions across multiple iterations using the leave-one-out approach. After the model was trained and used to predict blood hemoglobin levels from previously unseen conjunctiva images, the results were analyzed to assess its effectiveness.

The Hb-specialized model, which was fine-tuned from the ViT-based patch16-224, did not achieve satisfactory results. A significant number of errors were observed, as reported in Table 1.

Table 2
Performance metrics of the final Hb-personalized model. The regression metrics evaluate the model's ability to estimate hemoglobin values, whereas the classification metrics assess its ability to detect anemia. Error values are expressed in g/dL.

Regression metrics	
Mean squared error (MSE)	0.20
Root mean squared error (RMSE)	0.44
Mean absolute error (MAE)	0.25
Coefficient of determination (R^2)	0.94
Classification metrics	
Sensitivity	1.0
Specificity	0.72
Positive predictive value (PPV)	0.96
Negative predictive value (NPV)	1.0
Accuracy	0.98

As shown in the table, the application of a subsequent fine-tuning step individually to each patient's image set led to a substantial reduction in the prediction error. This highlights the effectiveness of the Hb-personalized model in achieving more accurate hemoglobin estimations.

The metrics of the final Hb-personalized model are reported in Table 2.

The MSE of 0.20 and RMSE of 0.44 indicate that the model maintained a low prediction error when estimating hemoglobin levels from the conjunctival images. The MAE of 0.25 g/dL further confirms that, on average, the model's predictions deviated only slightly from actual laboratory values. These values suggest a high level of precision, especially considering that small variations in hemoglobin levels are clinically relevant.

Furthermore, the R^2 of 0.94 demonstrates that the model explained 94% of the variance in actual hemoglobin values, which indicates its reliability in predicting hemoglobin levels from noninvasive imaging data. This result significantly surpasses those of previous models in the literature, where lower R^2 values indicate weaker correlations between predicted and actual hemoglobin levels.

Beyond numerical estimation, the model's performance in classifying anemia was equally impressive. The sensitivity of 1.0 demonstrates that the model correctly identified all anemic individuals, thus ensuring that there were no false-negatives. This is a crucial feature for any diagnostic tool, as missing an anemia case could lead to delayed treatment and potential health complications. Although the specificity was slightly lower at 0.72, which indicates that 72% of nonanemic

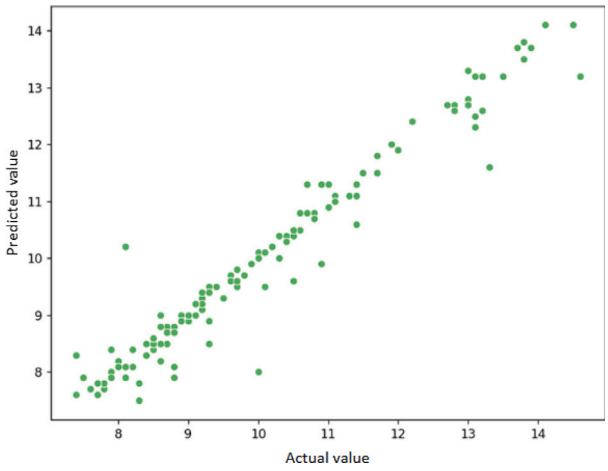

Fig. 10. Scatter plot that compares the actual and predicted hemoglobin values. The alignment along the diagonal indicates that the model accurately follows the expected trend, with minimal deviations suggesting that there are no systematic errors or bias in predictions.

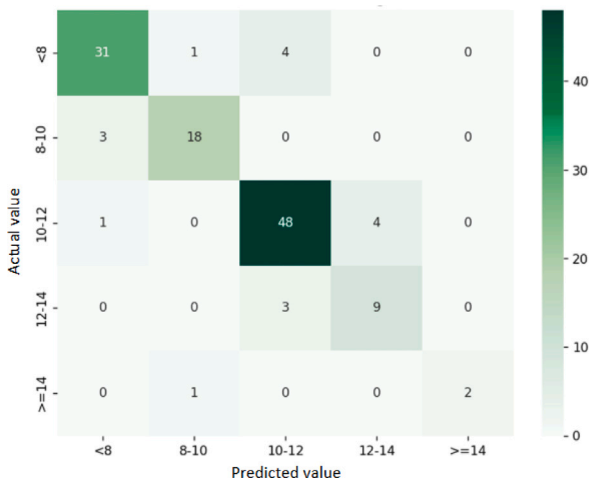

Fig. 11. Confusion matrix that categorizes hemoglobin predictions into predefined ranges. The strong concentration along the diagonal highlights the model's ability to classify hemoglobin levels correctly, with only a few misclassifications. The low frequency of severe errors suggests robustness and good generalization ability on test data.

individuals were correctly classified, this trade-off is often acceptable in medical applications where the priority is to avoid missing true cases of anemia rather than minimizing false alarms.

The model also achieved a PPV of 0.96, which indicates that when it identified a patient as anemic, there was a 96% probability that the diagnosis was correct. This high precision reduces the likelihood of unnecessary medical interventions due to false-positive results. Additionally, the NPV of 1.0 indicates that all nonanemic individuals were accurately identified, thus ensuring that no healthy patient was misclassified as anemic. The overall accuracy of 98% further supports the model's reliability by showing that the vast majority of predictions matched the actual clinical condition of the patients, as confirmed by laboratory blood test results.

The visual representations (Figs. 10 and 11 further support these findings. A comparison between the predicted and actual values reveals that the model effectively followed the correct trend in hemoglobin levels. The errors are limited in distribution and do not exhibit systematic patterns, which indicates that there was no inherent bias in the model. The confusion matrix suggests that significant misclassifications were rare. Additionally, the low frequency of severe errors indicates that the model did not suffer from overfitting and maintained good generalizability to the test data.

An analysis of the results from various studies reveals that our model outperformed previous approaches across almost all key metrics. Table 3 presents a comparison between our study and other experiments discussed in Section 2, which highlights the improvements introduced by the Hb-personalized model.

Our model achieves an R^2 of 0.94, thus outperforming other regression-based approaches such as those of Park et al. (2020) [16] (0.912), Ghosal et al. (2020) [19] (0.8774), and Anggraeni et al. (2017) [18] (0.8139). This finding indicates that our model better explains the variance in Hb levels, thereby resulting in more reliable predictions.

From a classification standpoint, our model attained an accuracy of 98%, which was significantly higher than those of other studies, such as Suneret al. (2021) [17] (82.9%), Dimauro et al. (2023) [22] (87%), and Appiahene et al. (2023) [23] (84.79%). Moreover, the sensitivity of 100% exceeds those of several previous studies, such as Suner et al. (2021) [17] (90.7%), Dimauro et al. (2023) (64%), and Das et al. (2024) (75.8%). However, although our specificity (72%) was slightly lower than those of other studies (Kato et al. (2024) [25] (99%), Dimauro et al. (2023) [22] (93%)), our method achieved a balanced trade-off between correctly identifying anemic and nonanemic individuals.

With respect to the error metrics, our model yielded a significantly lower MAE of 0.25 g/dL and RMSE of 0.44 g/dL, thus outperforming Kasiviswanathan et al. (2020) [20] (1.34 g/dL, 1.72 g/dL) and Appiahene et al. (2023) [23] (1.50 g/dL, -). These improvements indicate that our model provides more precise Hb estimations, thus reducing deviations from actual values.

Overall, these findings suggest that the Hb-personalized model achieves superior performance in both regression and classification tasks, which makes it a highly reliable and clinically viable tool for noninvasive Hb estimation. The combination of high accuracy, exceptional sensitivity, and minimal prediction errors has improved upon previous state-of-the-art approaches.

This project has led to the development of an advanced model for hemoglobin-level prediction that achieves superior accuracy and performance compared with those of previous studies. The integration of ViT techniques and the personalization of the model for individual patients yielded highly promising results, with an R^2 of 0.94 and an accuracy of 98%. These values indicate that the model provides precise predictions with minimal errors, which makes it particularly suitable for applications that require reliable and continuous hemoglobin level assessments.

A key strength of this work lies in the model's ability to offer a noninvasive measurement method, which reduces the need for frequent blood draws. This is particularly advantageous for patients who require continuous hemoglobin monitoring, such as individuals with chronic anemia, kidney disease, and hematological disorders, pregnant women, and oncology patients. Additionally, its high sensitivity (100%) ensures that anemic individuals are correctly identified, which minimizes the risk of missed diagnoses. Importantly, even laboratory hemoglobin measurements have a natural variance of 2%–5%, which indicates that some level of imprecision is inherent in standard clinical methods.

An innovative aspect of this project is the personalized approach, which has not been previously explored in the literature for hemoglobin estimation. Unlike those of existing studies, this model requires fine-tuning for each patient to adapt to their individual physiological characteristics. While this limits large-scale applicability, as it necessitates patient-specific training, the exceptionally high accuracy achieved suggests its potential clinical utility, especially for patients who require frequent and precise monitoring. Furthermore, the fine-tuning process is remarkably fast and requires only four images per patient and minimal computational resources.

Table 3
Comparison of the Hb-personalized model with models from previous studies in terms of regression and classification performance. The table includes R^2 values for the regression-based models and accuracy, sensitivity, specificity, MAE, and RMSE values for the classification-based approaches. Our model demonstrates superior predictive accuracy by achieving the highest R^2 and accuracy, along with significantly lower MAEs and RMSEs, which indicate improved precision in Hb estimation and anemia classification.

Study	R^2	Accuracy (%)	Sensitivity (%)	Specificity (%)	MAE (g/dL)	RMSE (g/dL)
Hb-personalized (Our model)	**0.94**	**98.0**	**100.0**	72.0	**0.25**	**0.44**
Park et al. (2020) [16]	0.912	–	–	–	–	–
Suner et al. (2021) [17]	–	82.9	90.7	73.3	–	–
Anggraeni et al. (2017) [18]	0.8139	–	–	–	–	–
Ghosal et al. (2020) [19]	0.8774	–	–	–	–	–
Kasiviswanathan et al. (2020) [20]	–	–	–	–	1.34	1.72
Ghosal et al. (2021) [21]	–	–	90.0	–	–	–
Dimauro et al. (2023) [22]	–	87.0	64.0	93.0	–	–
Appiahene et al. (2023) [23]	–	84.79	83.5	–	1.50	–
Camporeale et al. (2022) [24]	–	69.0	69.0	87.0	–	–
Kato et al. (2024) [25]	0.44	–	20.0	**99.0**	–	–
Das et al. (2024) [26]	–	–	75.8	90.0	–	–

From a practical perspective, the model could be integrated into a medical device or a mobile application capable of real-time analysis of ocular images. This would enable rapid and cost-effective screening, improve accessibility to anemia diagnosis and reduce health care costs. Such technology could facilitate home-based monitoring, which would benefit both patients and the health care system by enabling early detection and timely interventions.

Notwithstanding the excellent results reported in this study, it is important to acknowledge potential limitations that may affect the robustness and generalizability of the proposed model.

The estimation of hemoglobin levels from palpebral conjunctiva images relies on indirect visual cues, such as pallor or redness, which reflect physiological manifestations of anemia but do not measure hemoglobin concentration directly. While the hemoglobin labels were obtained from laboratory tests conducted during the same clinical session as image acquisition, minor fluctuations in clinical measurements are still possible, partly due to the tolerance range of the laboratory measuring instruments and may introduce noise into the regression targets. Despite this, numerous studies in recent years have consistently confirmed that the palpebral conjunctiva, to the best of our knowledge, is the only external human tissue that allows a reasonable estimate of anemia status. The main reason is that the palpebral conjunctiva mucosa is rich in directly visible blood vessels, is not affected by skin color, and is not significantly influenced by factors such as fever, age, or ethnicity. The only interfering factor is related to ocular pathologies.

Another critical aspect is the inherently non-linear relationship between visual signs and hemoglobin concentration. In borderline anemia cases or individuals with chronic physiological adaptation, visual cues may be subtle, inconsistent, or clinically ambiguous, potentially leading to less accurate predictions near clinical thresholds.

The dataset used in this study is relatively small and exhibits a slight imbalance toward lower hemoglobin values. Although the dual fine-tuning approach and leave-one-out cross-validation were implemented to reduce overfitting and enhance personalization, the limited size and diversity of the dataset may constrain the model's ability to generalize to broader populations. Future studies should validate the proposed method on larger and more heterogeneous cohorts. It is important to note that many patients (e.g., those with oncological diseases) can have fast (2–3 weeks) and significant changes in hemoglobin concentration (1–3 g/dL; it can also drop below 8 g/dL) due to chemotherapy and, since our study is patient-specific, we are moderately optimistic that our system could serve as a valuable decision-support tool.

Moreover, although our training strategy was designed to mitigate architectural limitations of Vision Transformers, the absence of convolutional inductive priors, such as locality and translation invariance, could still affect model stability in particularly noisy or atypical scenarios.

In conclusion, the model developed in this project has potential as a clinical support tool for noninvasive hemoglobin monitoring. With further large-scale validation and the development of dedicated applications, it could become a viable alternative to traditional blood tests and could facilitate continuous hemoglobin monitoring for patients who require frequent assessments.

CRediT authorship contribution statement

Mauro Camporeale: Writing – review & editing, Software. **Felice Clemente:** Data curation, Resources. **Giovanni Dimauro:** Supervision, Conceptualization, Writing – original draft, Writing – review & editing. **Nunzia Lomonte:** Writing – review & editing, Writing – original draft, Visualization, Validation, Methodology, Conceptualization, Investigation. **Rosalia Maglietta:** Formal analysis, Validation. **Crescenza Pasciolla:** Resources, Validation. **Davide Sacco:** Writing – original draft, Validation, Software, Data curation, Investigation, Visualization. **Gian Maria Zaccaria:** Resources, Data curation.

Informed consent and patient details

The authors declare that they obtained a written informed consent from the patients and/or volunteers included in the article and that this report does not contain any personal information that could lead to their identification.

Human and animal rights

The authors declare that the work described has been carried out in accordance with the Declaration of Helsinki of the World Medical Association revised in 2013 for experiments involving humans as well as in accordance with the EU Directive 2010/63/EU for animal experiments.

Funding

This work did not receive any grant from funding agencies in the public, commercial, or not-for-profit sectors.

Declaration of competing interest

The authors declare that they have no known competing financial interests or personal relationships that could have appeared to influence the work reported in this paper.

References

[1] E. McLean, M. Cogswell, I. Egli, D. Wojdyla, B. de Benoist, Worldwide prevalence of anaemia, WHO vitamin and mineral nutrition information system, 1993–2005, Public Heal. Nutr. 12 (4) (2009) 444–454, http://dx.doi.org/10.1017/S1368980008002401.

[2] G.A. Stevens, M.M. Finucane, L.M. De-Regil, C.J. Paciorek, S.R. Flaxman, F. Branca, J.P. Peña-Rosas, Z.A. Bhutta, M. Ezzati, Nutrition Impact Model Study Group (Anaemia), Global, regional, and national trends in haemoglobin concentration and prevalence of total and severe anaemia in children and pregnant and non-pregnant women for 1995–2011: a systematic analysis of population-representative data, Lancet Glob Heal. 1 (1) (2013) e16–25.

[3] G.A. Stevens, C.J. Paciorek, M.C. Flores-Urrutia, E. Borghi, S. Namaste, J.P. Wirth, P.S. Suchdev, M. Ezzati, F. Rohner, S.R. Flaxman, L.M. Rogers, National, regional, and global estimates of anaemia by severity in women and children for 2000-19: a pooled analysis of population-representative data, Lancet Glob Heal. 10 (5) (2022) e627–e639.

[4] E. McLean, M. Cogswell, I. Egli, D. Wojdyla, B. de Benoist, Worldwide prevalence of anaemia, WHO vitamin and mineral nutrition information system, 1993–2005, Public Heal. Nutr. 12 (4) (2008) 444–454.

[5] K.V. Patel, Epidemiology of anemia in older adults, Semin. Hematol 45 (4) (2008) 210–217.

[6] J. White, M. Anna, Blood and bone marrow pathology, Elsevier, 2011.

[7] M.G. Camporeale, L. Colizzi, N. Lomonte, A. Ragone, Development of a desktop application to enable doctors to remotely monitor patients' hematological parameters, in: International Conference on Product-Focused Software Process Improvement, Springer, 2023, pp. 48–59.

[8] V.S. Barletta, M.G. Camporeale, N. Lomonte, M. Scalera, E. Gentile, DeskEmo, a multi-platform desktop software for remote control and monitoring of hematological parameters, in: Italian Forum of Ambient Assisted Living, Springer, 2023, pp. 224–232.

[9] G. Dimauro, S. De Ruvo, F. Di Terlizzi, A. Ruggieri, V. Volpe, L. Colizzi, F. Girardi, Estimate of anemia with new non-invasive systems—A moment of reflection, Electronics 9 (5) (2020) http://dx.doi.org/10.3390/electronics9050780, URL https://www.mdpi.com/2079-9292/9/5/780.

[10] M.F. Young, K. Raines, F. Jameel, M. Sidi, S. Oliveira-Streiff, P. Nwajei, K. McGlamry, J. Ou, A. Oladele, P.S. Suchdev, Non-invasive hemoglobin measurement devices require refinement to match diagnostic performance with their high level of usability and acceptability, PLoS One 16 (7) (2021) e0254629.

[11] P. Appiahene, J.W. Asare, E.T. Donkoh, G. Dimauro, R. Maglietta, Detection of iron deficiency anemia by medical images: a comparative study of machine learning algorithms, BioData Min. 16 (1) (2023) 1–20.

[12] C.I. Sanchez-Carrillo, Bias due to conjunctiva hue and the clinical assessment of anemia, J. Clin. Epidemiol. 42 (8) (1989) 751–754.

[13] T.N. Sheth, N.K. Choudhry, M. Bowes, A.S. Detsky, The relation of conjunctival pallor to the presence of anemia, J. Gen. Intern. Med. 12 (2) (1997) 102–106.

[14] S. Suner, G. Crawford, J. McMurdy, G. Jay, Non-invasive determination of hemoglobin by digital photography of palpebral conjunctiva, J. Emerg. Med. 33 (2) (2007) 105–111.

[15] B. Babenko, I. Traynis, C. Chen, P. Singh, A. Uddin, J. Cuadros, L.P. Daskivich, A.Y. Maa, R. Kim, E.Y.-C. Kang, et al., A deep learning model for novel systemic biomarkers in photographs of the external eye: a retrospective study, Lancet Digit. Heal. (2023).

[16] S.M. Park, M.A. Visbal-Onufrak, M.M. Haque, M.C. Were, V. Naanyu, M.K. Hasan, Y.L. Kim, Mhealth spectroscopy of blood hemoglobin with spectral super-resolution, Optica 7 (6) (2020) 563–573.

[17] S. Suner, J. Rayner, I.U. Ozturan, G. Hogan, C.P. Meehan, A.B. Chambers, J. Baird, G.D. Jay, Prediction of anemia and estimation of hemoglobin concentration using a smartphone camera, PloS One 16 (7) (2021) e0253495.

[18] M. Anggraeni, A. Fatoni, Non-invasive self-care anemia detection during pregnancy using a smartphone camera, in: IOP Conference Series: Materials Science and Engineering, vol. 172, (1) IOP Publishing, 2017, 012030.

[19] S. Ghosal, D. Das, V. Udutalapally, A.K. Talukder, S. Misra, sHEMO: Smartphone spectroscopy for blood hemoglobin level monitoring in smart anemia-care, IEEE Sensors J. 21 (6) (2020) 8520–8529.

[20] S. Kasiviswanathan, T.B. Vijayan, S. John, Ridge regression algorithm based non-invasive anaemia screening using conjunctiva images, J. Ambient. Intell. Humaniz. Comput. (2020) 1–11.

[21] S. Ghosal, D. Das, V. Udutalapally, P. Wasnik, iNAP: A hybrid approach for NonInvasive anemia-polycythemia detection in the iomt, 2021, http://dx.doi.org/10.1145/3503466.

[22] G. Dimauro, M.E. Griseta, M.G. Camporeale, F. Clemente, A. Guarini, R. Maglietta, An intelligent non-invasive system for automated diagnosis of anemia exploiting a novel dataset, Artif. Intell. Med. 136 (2023) 102477.

[23] P. Appiahene, K. Chaturvedi, J.W. Asare, E.T. Donkoh, M. Prasad, Cp-anemic: A conjunctival pallor dataset and benchmark for anemia detection in children, Med. Nov. Technol. Devices (2023) 100244.

[24] G. Dimauro, M.G. Camporeale, A. Dipalma, A. Guarini, R. Maglietta, Anaemia detection based on sclera and blood vessel colour estimation, Biomed. Signal Process. Control. 81 (2023) 104489, http://dx.doi.org/10.1016/j.bspc.2022.104489, URL https://www.sciencedirect.com/science/article/pii/S1746809422009430.

[25] S. Kato, K. Chagi, Y. Takagi, M. Hidaka, S. Inoue, M. Sekiguchi, N. Adachi, K. Sato, H. Kawai, M. Kato, Machine/deep learning-assisted hemoglobin level prediction using palpebral conjunctival images, Br. J. Haematol. 205 (4) (2024) 1590–1598.

[26] S. Das, F. Ahamed, A. Das, D. Das, J. Nandi, K. Banerjee, Niada (non-invasive anemia detection app), a smartphone-based application with artificial intelligence to measure blood hemoglobin in real-time: a clinical validation, Cureus 16 (7) (2024).

[27] S. Kasiviswanathan, T. Bai Vijayan, L. Simone, G. Dimauro, Semantic segmentation of conjunctiva region for non-invasive anemia detection applications, Electronics 9 (8) (2020) http://dx.doi.org/10.3390/electronics9081309, URL https://www.mdpi.com/2079-9292/9/8/1309.

[28] G. Dimauro, L. Simone, Novel biased normalized cuts approach for the automatic segmentation of the conjunctiva, Electronics 9 (6) (2020) http://dx.doi.org/10.3390/electronics9060997, URL https://www.mdpi.com/2079-9292/9/6/997.

[29] S.P. Dakua, J.S. Sahambi, LV contour extraction from cardiac MR images using random walks approach, in: 2009 IEEE International Advance Computing Conference, IEEE, 2009, pp. 228–233.

[30] S. Dakua, J. Sahambi, Automatic contour extraction of multi-labeled left ventricle from cmr images using CB and random walk approach, Cardiovasc. Eng 10 (1) (2010) 30–43.

[31] S.P. Dakua, Performance divergence with data discrepancy: a review, Artif. Intell. Rev. 40 (4) (2013) 429–455.

[32] C.R. Harris, K.J. Millman, S.J. van der Walt, R. Gommers, P. Virtanen, D. Cournapeau, E. Wieser, J. Taylor, S. Berg, N.J. Smith, R. Kern, M. Picus, S. Hoyer, M.H. van Kerkwijk, M. Brett, A. Haldane, J.F. del Río, M. Wiebe, P. Peterson, P. Gérard-Marchant, K. Sheppard, T. Reddy, W. Weckesser, H. Abbasi, C. Gohlke, T.E. Oliphant, Array programming with NumPy, Nature 585 (7825) (2020) 357–362, http://dx.doi.org/10.1038/s41586-020-2649-2, URL https://doi.org/10.1038/s41586-020-2649-2.

[33] W. McKinney, Data structures for statistical computing in python, in: S. van der Walt, J. Millman (Eds.), Proceedings of the 9th Python in Science Conference, 2010, pp. 56–61, http://dx.doi.org/10.25080/Majora-92bf1922-00a.

[34] A. Paszke, S. Gross, F. Massa, A. Lerer, J. Bradbury, G. Chanan, T. Killeen, Z. Lin, N. Gimelshein, L. Antiga, A. Desmaison, A. Kopf, E. Yang, Z. DeVito, M. Raison, A. Tejani, S. Chilamkurthy, B. Steiner, L. Fang, J. Bai, S. Chintala, Pytorch: An imperative style, high-performance deep learning library, Adv. Neural Inf. Process. Syst. 32 (2019) URL https://pytorch.org/.

[35] T. Wolf, L. Debut, V. Sanh, J. Chaumond, C. Delangue, A. Moi, P.-E. Roussel, R. Louf, M. Funtowicz, J. Phang, T. Faucon, J. Brew, A.M. Rush, Transformers: State-of-the-art natural language processing, 2020, https://arxiv.org/abs/1910.03771. (Accessed 27 February 2025).

[36] A. Al-Kababji, F. Bensaali, S.P. Dakua, Y. Himeur, Automated liver tissues delineation techniques: a systematic survey on machine learning current trends and future orientations, Eng. Appl. Artif. Intell. 117 (2023) 105532.

[37] M.Y. Ansari, I.A.C. Mangalote, D. Masri, S.P. Dakua, Neural network-based fast liver ultrasound image segmentation, in: 2023 International Joint Conference on Neural Networks, IJCNN, IEEE, 2023, pp. 1–8.

[38] S.-R. Pasricha, K. Colman, E. Centeno-Tablante, M.-N. Garcia-Casal, J.-P. Peña-Rosas, Revisiting WHO haemoglobin thresholds to define anaemia in clinical medicine and public health, Lancet. Haematol. 5 (2) (2018) e60–e62.